Pergamon

Journal of Structural Geology, Vol. 16, No. 9, pp. 1259 to 1273, 1994

0191-8141/94 $07.00+0.00

0191-8141(93)E0024-F

Quantitative analysis of populations of small faults

ROB WESTAWAY

16 Neville Square, Durham DH1 3PY, U.K.

(*Received* 17 *December* 1992; *accepted in revised form* 16 *November* 1993)

Abstract—Tectonic strain includes contributions from small faults, with length less than the thickness of the brittle upper crust. This study derives algebra to determine the strain associated with small faults that follow a power-law (i.e. fractal) distribution, independent of assumptions concerning how they relate to large faults in the same region, and discusses how to apply this algebra for a range of small fault sample types. The method is illustrated using as case studies the Jurassic extension in the North Sea, the Miocene and younger extension in the Gulf of Suez, and the Hercynian strike-slip faulting the Badajoz–Cordoba fault zone in southern Spain. My preferred estimates for the strain accommodated on small normal faults, with length <10 km, are ~0.04 in the North Sea and ~0.1 in the Gulf of Suez: ~20 and ~30% of the overall extensional strain in each region. This estimate makes the percentage of strain accommodated on small faults in the North Sea smaller than values in studies that assume that a single power law fits both small and large faults. My preferred estimate for the strain accommodated on small strike-slip faults in the Badajoz–Cordoba fault zone is ~0.3, which may be ~75% of the overall strain accommodated in this zone. These faults are more closely packed than the normal faults in the other localities.

INTRODUCTION

LARGE faults, which cut the brittle upper crust, are sufficiently sparse in most regions that the strain contribution from each can be estimated individually. Most regions also contain many small faults, with length less than the thickness of the brittle upper crust. Their strain contribution can be added to that of the large faults to give the overall strain from faulting. Such an estimate can in principle be compared with independent estimates of strain, for example from crustal thickening or thinning, to quantify the importance of faulting during tectonic deformation.

Although simple in principle, in practice the comparison of independent estimates of strain has for many years been controversial. Some studies argue that large faults take up most strain, and with a minor addition to cover small faults, can match independent estimates of strain. However, others (e.g. Ziegler 1983) have noticed apparent 'extension discrepancies' in extensional provinces, asserting that the contribution from large normal faults may dramatically underestimate the extensional strain. It has been suggested that small faults may account for these discrepancies (e.g. Marrett & Allmendinger 1992).

Quantifying strain associated with small faults is complicated by effects of sampling. It is not usually possible to sample small faults in three dimensions; sampling is instead usually only possible in one or two dimensions. It is thus necessary to have the algebraic means to quantify the three-dimensional fault population in any region from one-dimensional or two-dimensional studies. Some past studies (e.g. Scholz & Cowie 1990, Marrett & Allmendinger 1991, 1992, Walsh *et al.* 1991, Jackson & Sanderson 1992) have published algebra for their particular sampling style. However, this has either been normalized to compare strain contributions for faults of different sizes or expressed in terms of arbitrary size limits of faults (rather than the limit at the transition from small to large faults). The absence of appropriate theory has made it difficult to resolve the conflicting viewpoints concerning the importance of small faults.

This study presents algebra to quantify numbers and absolute strain contributions of small faults, and illustrates its application—including potential pitfalls that may arise–using appropriate case studies. It thus differs from other studies that determine strain contributions for small faults as a proportion of the contribution from the large faults in the same region, without calculating the strain associated with faults in either size range. First, algebra is derived to give strain for populations of small faults. Second, algebra is derived to interrelate distributions of small faults obtainable with different sampling geometries. Third, the algebra is used to analyse, as case studies, the data sets of Heffer & Bevan (1990) for faults in the Gulf of Suez, Walsh *et al.* (1991) for faults beneath the North Sea, and Jackson & Sanderson (1992) for the Badajoz–Cordoba fault zone in southern Spain.

ANALYSIS OF POPULATIONS OF SMALL FAULTS

Previous work relating displacement, length and numbers of faults

Past studies relating fault length L and displacement D usually suggest power laws with

$$D = BL^n, \quad (1)$$

Table 1. Notation

Term	Units	Meaning
L	m	Fault length
L_{min}	m	Minimum length of small faults in a region
L_0	m	Maximum length of small faults in a region
L_{max}	m	Maximum length of large faults in a region
D	m	Fault displacement
W	m	Length of region where fault sampling is carried out
J	m	Width of region where fault sampling is carried out
H	m	Vertical extent of region where fault sampling is carried out
e	dimensionless	Strain
M_g	m^3	Geometric moment
n	dimensionless	Exponent in power law linking L and D
B	m^{-n+1}	Scale factor in power law linking L and D
N	dimensionless	Number of faults in a given three-dimensional sample above a given L or D
c	dimensionless	Exponent in power law linking N and D
a	m^{c-3}	Scale factor in power law linking N and D
N_2	dimensionless	Number of faults in a given two-dimensional sample above a given L or D
c_2	dimensionless	Exponent in power law linking N_2 and D
a_2	m^{c_2-2}	Scale factor in power law linking N_2 and D
N_1	dimensionless	Number of faults in a given one-dimensional sample above a given L or D
c_1	dimensionless	Exponent in power law linking N_1 and D
a_1	m^{c_1-1}	Scale factor in power law linking N_1 and D
p_1	dimensionless	Probability that a fault is sampled in one-dimensional sampling
p_2	dimensionless	Probability that a fault is sampled in two-dimensional sampling
y_0	m^{nc_2-2}	Constant of proportionality in incremental fault number-density distributions
δL	m	Range of L in incremental fault number-density distributions
k	dimensionless	Ratio of δL to L

where B and n are constants. This empirical fitting of observations of fault size is sometimes used as evidence for self-similar fault growth. Walsh & Watterson (1987, 1988) suggested $n = 2$, consistent with self-similar growth where D increases by the same amount each time the fault slips. Others (e.g. Marrett & Allmendinger 1991) have suggested $n \sim 1.5$ instead, consistent with self-similar growth where each time the fault slips the increment to D is proportional to the number of times the fault has slipped. Marrett & Allmendinger (1991) determined $n = 1.46$ and $B = 8.91 \times 10^{-3}$ $km^{-0.46}$, which predicts that a fault with $L = 1$ km will have $D \cong 9$ m. Scholz & Cowie (1990) suggested instead that n is $\cong 1$, with B dimensionless. They argued that B may be as high as 0.01, such that a typical fault with $L = 1$ km will have $D = 10$ m; a similar value.

Much of the recent literature has adopted notation where $N(D)$ denotes the cumulative number of faults in a given volume with displacement no less than D (Tables 1 and 2). $N(D)$ is regarded as proportional to D raised to the power of $-c$, or $N \propto D^{-c}$, where c is a positive number. Assuming faults are uniformly distributed in position, the number in a cuboid of upper crust with width W, length J and thickness H will also be proportional to its volume, WJH. These proportionalities can be converted into an equation by introducing a constant of proportionality a, such that

$$N(D) = aHWJD^{-c}. \quad (2)$$

The units of a are length to the power of $c - 3$, and are thus dimensionless if $c = 3$.

This use of a constant of proportionality implicitly assumes that the distribution of small faults is open-ended, and thus applicable to faults with arbitrarily large displacement and length. However, no real population of small faults can be open-ended, because the thickness of the brittle upper crust limits their length. Appendix 2 shows that use of a distribution of the form of equation (2) for small faults can lead to inconsistent results if combined with the assumption of an upper size-limit. However, if one is careful one can avoid the errors in logic that follow from inconsistent assumptions, and derive valid equations that enable populations of small faults to be quantified using cumulative distributions.

Effects of sampling cause additional complications. One is usually obliged to sample small faults either in two dimensions, for example from a map, or in one dimension, for example by noting faulted offsets of a reflector on a seismic section. Several studies (e.g. Heffer & Bevan 1990, Walsh *et al.* 1991, Jackson &

Table 2. Comparison of notations

Parameter	S	M	W	J
D	D	d	D	d
L	L	l	L	(2)
n	(1)	C_2	n	(2)
B	γ^*	(1)	c	(2)
c_1	(2)	C_1''	S	(2)
c_2	(2)	C_1'	(2)	(2)
c	C_1	C_1	(2)	D
nc	C	C_1C_2	(2)	(2)

S, M, W. and J denote Scholz & Cowie (1990), Marrett & Allmendinger (1991), Walsh *et al.* (1991), and Jackson & Sanderson (1992). Note (1) indicates that the study did not use an algebraic symbol, but instead assumed a constant value for this parameter. Note (2) indicates that the study did not use this parameter, and so did not define its symbol. Because the same letters are used for different parameters in different notations, there is great potential for confusion if one is not careful.

Sanderson 1992) have noted practical difficulties with some sampling methods. This study is not concerned with such difficulties; it instead addresses how to use samples of fault populations once the sampling has been carried out.

One- or two-dimensional sampling will miss small faults with increasing probability as their length decreases, because they do not intersect the sampling line or plane. They will thus cause different power laws between numbers of faults sampled and D (e.g. Marrett & Allmendinger 1991), with cumulative numbers $N_1(D)$ and $N_2(D)$ and exponents c_1 and c_2 for one- and two-dimensional samples (see Appendix 1). Values of c can be estimated for small faults that are in part missed in one- and two-dimensional sampling as:

$$c = c_1 + 2/n \tag{3}$$

$$c = c_2 + 1/n. \tag{4}$$

Geometric moment, M_g, is a scalar measure of the deformation associated with any fault, defined as the product of D and its area. The finite thickness H of the brittle layer, typically ~10 km, affects how M_g scales with L. For faults that cut the brittle layer,

$$M_g = DLH \tag{5}$$

(e.g. Scholz & Cowie 1990) but for small square equidimensional faults.

$$M_g = DL^2. \tag{6}$$

If instead small faults are circular with diameter L, then

$$M_g = (\pi/4)DL^2. \tag{7}$$

Small faults are assumed square throughout this study, because of the greater difficulty of sampling them when other shapes are assumed. For example, if they are assumed circular, L varies with distance of the sample line from the mid-point of the fault (e.g. Heffer & Bevan 1990).

Displacement will in general vary across any fault plane, decreasing to zero at its edges. Because most of this decrease is usually near these edges, average displacement is typically not much less than maximum displacement. Unless one by chance samples near an edge of a fault, an arbitrary displacement sample will thus typically not differ much from the maximum or average value. In equations (5)–(7) D is average displacement; in (1) and (2) D is the arbitrary sample where the sample line or plane crosses the fault. Marrett & Allmendinger (1990) argued that assuming a given random sample indicates average displacement will typically cause minimal error. This study adopts their view, treating these quantities as equivalent.

Previous work on strain associated with populations of small faults

Scholz & Cowie (1990) calculated cumulative M_g of small faults, ΣM_g, assuming that D and L are related using equation (2), by integrating M_g as a function of fault size treating the faults as a continuous distribution with L up to L_0. Assuming small faults are square, when generalized for equation (1) instead this relation gives (see Appendix 1):

$$\Sigma M_g = \frac{aB^{1-c}cWJHL_0^{2+n-nc}}{2+n-nc}. \tag{8}$$

The strain tensor $\varepsilon_{i,j}$ associated with these faults can be calculated using Kostrov's (1974) method. If the scalar geometric moment is replaced by elements of a geometric moment tensor $M_{gi,j}$ $(i,j = 1,3)$ using information on the fault orientations and slip senses, then

$$\varepsilon_{i,j} = \frac{\Sigma M_{gi,j}}{2WJH}. \tag{9}$$

The orientation of the principal axes, or eigenvectors, of this tensor will depend on the orientations and slip senses of individual faults within the deforming region. For example, if a region contains a set of dip-slip faults with dip of 45°, which take up either extension or shortening, the horizontal eigenvectors will be associated with an eigenvalue that gives the extensional (or shortening) strain, ε. The value of ε can then be determined from the sum of scalar geometric moments ΣM_g (see e.g. Westaway 1992a):

$$\varepsilon = \frac{\Sigma M_g}{2WJH}. \tag{10}$$

When typical fault dip δ is not 45°, the horizontal strain can be determined instead as:

$$\varepsilon = \frac{\Sigma M_g \sin(2\delta)}{2WJH} \tag{11}$$

(see e.g. Westaway 1992b). For extension on normal faults with dip δ, the extensional strain is thus:

$$\varepsilon = \frac{aB^{1-c}c \sin(2\delta)L_0^{2+n-nc}}{2(2+n-nc)}. \tag{12}$$

The amount of extension will equal εW provided $\varepsilon \ll 1$.

This reasoning assumes that populations of small faults follow power laws between L and D, and N and D. In (12) strain is proportional to a, indicating that it is impossible to quantify strain on small faults without knowledge of their number densities. Furthermore, because ε depends on M_g, and M_g depends on both L and D, ε has to be a function of both L and D. Any estimate that results for the strain accommodated by a population of small faults is thus subject to the use of some relation between L and D.

If one accepts that the overall faulted displacement across any profile equals the sum of displacements on faults within it (see e.g. Westaway & Kusznir 1993) then one-dimensional sampling of $N_1(D)$ can give the faulted displacement along any profile (e.g. Jackson & Sanderson 1992), and hence the strain, independent of the relation between fault displacement and length. How-

ever, this method does not reveal how much of this strain is associated with small faults. The limit of D for small faults depends on the brittle layer thickness via equation (1), and cannot be determined by one-dimensional sampling (see below, also Appendix 1).

Scholz & Cowie (1990) derived an analogous equation to (8) for large faults, assuming that equation (2) links L and D with $n = 1$. They estimated c for these faults as ~1.1 using data from an approximately 3000 km^2 locality in Japan where H is ~10 km. The largest fault has $L \cong 500$ km, and sampling appeared complete down to $L \sim 10$ km. They showed that with these parameters, the faults sampled accounted for over 95% of the estimated ΣM_g. Even if the largest fault had been only ~20 km long, according to fig. 3 of Scholz & Cowie (1990) faults with L ~10 km or more would account for ~80% of ΣM_g. Their results suggest that almost all the strain in this locality is associated with large faults and it is simple to correct for the small faults that are missed to get a reliable estimate of the overall strain. Many other studies have numerically modelled deformation, including extension, assuming it is taken up on a limited number of large faults (e.g. Kusznir *et al.* 1991). The impressive match that can be obtained between observations and these models suggests strongly that not much strain is associated with smaller faults that are omitted from the modelling.

Walsh *et al.* (1991) suggested that c derived from the two-dimensional sampling by Scholz & Cowie (1990) should be corrected using equation (4) to give the true three-dimensional fault distribution. However, because Scholz & Cowie's (1990) c value was derived for faults with $L \gtrsim 10$ km, which most likely cut the brittle layer, it is wrong to make such a correction to their data set: for these large faults the three-dimensional exponent c will equal the exponent from the lower-dimensionality sample. Marrett & Allmendinger (1991) also showed that the method of Scholz & Cowie (1990) gives only an approximate result, because it treats the faults as a continuous distribution right up to the largest fault. Marrett & Allmendinger (1991) calculated ΣM_g instead treating the largest faults individually and the others as a continuum. They showed that this gives greater moment associated with the largest faults. They also suggested that their n value of ~1.5 was more appropriate than the value of ~1 that Scholz & Cowie (1990) used. Increasing n (keeping c, B and L_0 constant) will in general increase ΣM_g for a population of small faults. However, the different values of B associated with different n may counteract this effect, causing smaller ΣM_g for larger values of n. One of the case study localities discussed later (the Gulf of Suez) indeed shows smaller strain for larger n. Neither the use of $n > 1$, nor the individual treatment of the largest faults, nor consideration of the sampling geometry (given that $L \gtrsim 10$ km), thus necessarily invalidate Scholz & Cowie's (1990) conclusion that most geometrical moment in a region may be associated with the largest faults there.

Walsh *et al.* (1991) deduced that c is ~2–3 for normal faults that took up late Jurassic extension in the northern North Sea, with heave and throw (vertical component of D) ~1 mm to ~0.5 km. They adopted the relation for $D(L)$ from Marrett & Allmendinger (1991), which gives $L \sim 15$ km for $D \sim 0.5$ km. Except for a few of the largest faults that they considered, their sample thus had $L < H$ and thus required correction for the one-dimensional sampling. They obtained samples of $N_1(D)$ from seismic sections (for $D \gtrsim 10$ m) and boreholes (for $D \lesssim 0.01$ m), which both fit $c_1 = 0.8$. They then corrected c_1 using equation (3) to give c. With $n = 1$, c would be ~2.8, and with $n = 1.5$, c would be ~2.1. Assuming a self-similar distribution with these larger c values, they deduced that the proportion of strain associated with small faults is much larger than Scholz & Cowie (1990) concluded. Walsh *et al.* (1991) showed that with $c_1 = 0.8$ and the largest heave of 5 km, if the smallest heave considered is 0.1 km, near the limit of resolution on their seismic sections, almost half the likely total geometric moment of small faults is missed. They thus assumed self-similarity with the same power-laws for $N(D)$ and $D(L)$ for both large and small faults, although they calculated M_g appropriately for the two populations and treated the largest faults individually. They estimated that small faults, many of which are below the limit of resolution on seismic sections, probably account for 40% of the extension across the North Sea. Marrett & Allmendinger (1992) reached similar conclusions, arguing that the proportion of strain associated with small faults may be up to 60%. Their results indicate that the extension across the North Sea is uncertain by >30% even after detailed analysis including correction for small faults. These results imply that it is futile to try to estimate strain from faulting in most other regions, which are less well documented.

Much of this work on fault sampling has assumed that a certain proportion of strain is associated with small faults, which is independent of the actual strain in any region. The debate has concerned whether this proportion is small (say ≲20–30%) or large. Westaway (1992a) suggested instead that this view may be mistaken. He pointed out that if the strain in any region is small, there is no reason why all of it need not be accommodated on small faults. Given that the upper size limit of small faults is fixed by the thickness of the brittle upper crust, as strain increases the number density of the faults, and/or their displacement to length ratio will need to increase. The small faults may eventually become so closely spaced that they will interact, linking up to form larger faults that may cut the brittle layer. If this alternative view is correct, the proportion of strain associated with small faults will vary between regions. The absolute strain accommodated on small faults may tend towards an upper limit, which is determined by their maximum number density (the parameter a in equation (12)). This may vary between regions, and possibly also between fault types. In order to investigate further whether this view is correct, it is necessary to investigate individual case study localities in more detail than has so far been attempted. New theory is also required to enable these localities to be analysed.

New theory for strain associated with populations of small faults

Assuming that a population of small faults obeys power laws for $N(D)$ and $D(L)$ as in equations (1) and (2), Appendix 1 derives relations between the one- and two-dimensional number-density parameters a_1 and a_2 and exponents c_1 and c_2, and the three-dimensional parameters a and c:

$$N_1(D) = a_1 W D^{-c_1} \tag{13}$$

and

$$N_2(D) = a_2 W J D^{-c_2}. \tag{14}$$

N_1 and N_2 are numbers of small faults with displacement no less than D in one- and two-dimensional samples across a zone with width J and length W. Appendix 1 gives the relations between a, a_1 and a_2. These depend on B and n, which are thus critical parameters: as well as relating L and D, they also affect values of a derived from observations of a_1 or a_2.

Appendix 1 shows that equation (12) can be converted into a form (equation A1.17) that depends only on D_0 and parameters from the one-dimensional sample (see also Jackson & Sanderson 1992). This equation appears to be independent of B and n, and thus avoids contention as to their values. However, because L_0 establishes the upper limit of small faults, obtaining D_0 and L_0 requires equation (1). The strain contribution of small faults is thus not independent of B and n, as is expected given that strain depends on cumulative geometric moment, and geometric moment of each fault depends on both L and D. To make this explicit, (A1.17) can be adapted by substitution (using equation 1) to give the strain for small faults with dip δ and length $L_{min} = 0$ to L_0, sampled perpendicular to strike, as

$$\varepsilon = \frac{a_1 c_1 \cos(\delta) B^{1-c_1} L_0^{n(1-c_1)}}{(1-c_1)} \tag{15}$$

unless c_1 is precisely 1. Strain does depend on B and n, but B is to the power $1 - c_1$. With c_1 almost 1 the dependence of ε on L_0, B and n will be weak.

The strain, ε, associated with any given power-law distribution of small faults thus in general depends on L_0, a, B, c and n (see Appendix 1). When c is much smaller than 3, ε depends strongly on L_0. When c is almost 3, the dependence of ε on L_0 is weak (as noted by Walsh *et al.* 1991), and ε depends more strongly on a, B, c and n.

If $c_1 = 1$, $c_2 = 1 + 1/n$ or $c = 1 + 2/n$ (Appendix 1), an equal proportion of strain is associated with the small faults in each order-of-magnitude range of L, and the integral for strain would be infinite if the lower limit of L were zero. If any of these exponents is observed, integration must be truncated at a finite lower limit L_{min}. This may be ~1 mm, the typical grain size in many rock types (Walsh *et al.* 1991). Westaway (1992a) has shown that this distribution (with $n = 1$ and $c = 3$) is consistent with one of the simplest models for growth of populations of small faults (see also Sornette & Davy 1991). Because of this link with a simple model, my preference is to use $n = 1$ when estimating strain. However, when analysing observational case studies I also estimate strain using the alternative n value of 1.46 suggested by Marrett & Allmendinger (1991).

Appendix 1 thus addresses the estimation of strain accommodated by populations of small faults. It shows that consistent estimates can be obtained for different methods of sampling small faults. It also establishes how to convert between parameters estimated using different sampling methods, for instance how to calculate the parameters describing the three-dimensional distribution of small faults in a region from a one- or two-dimensional sample, and how to predict incremental fault distributions from cumulative distributions (and vice versa).

New theory for the spacing of small faults

It is important to have the means to estimate how closely spaced the faults of a given size are, in a region. Appendix 2 attempts to address spacings of small faults using parameters for cumulative distributions. Equation (A2.2) estimates the length W_1 of the one-dimensional sample line needed before one encounters a small fault with length L_0 or greater. Equation (A2.7) estimates the horizontal length W_2 perpendicular to fault strike of the two-dimensional sample plane needed before one encounters a small fault with length L_0 or greater. W_2 is always c_2/c_1 times W_1: the two are not consistent. Equation (A2.5) estimates the area A_2 of a vertical two-dimensional sample plane needed before one encounters a small fault with length L_0 or greater. Equation (A2.10) estimates the vertical cross-sectional area A_3 of the three-dimensional sample volume needed before one encounters a small fault with length L_0 or greater. A_3 is always c/c_2 times A_2: once again, the two are not consistent.

Appendix 3 shows instead that it is possible to obtain consistent results for fault spacings and number densities using incremental distributions. Equations (A3.11), (A3.6) and (A3.2) give number densities of faults with length around a particular value of L, from three-, two- and one-dimensional distributions. Appendix 3 shows explicitly that estimates derived using these equations from incremental distributions of different dimensionality are *always* consistent, regardless of the length of fault considered. However, when dealing with incremental distributions, one cannot estimate numbers of faults with precisely some particular length. One is obliged instead to estimate numbers of faults within some range of L, which I call δL, about the L value under consideration. One may either keep δL constant, regardless of L; or one may work in terms of δL keeping a constant proportion of L, using k to denote the ratio $\delta L/L$. Appendix 3 shows that these two methods of representing populations of small faults will result in different exponents in their incremental distributions.

It is now possible to see why many valid results for

Table 3. Distributions of small faults in the study regions

	c_1	c_2	c	a	δN (10 km)	δN (1 km)	δN (0.1 km)
			$n = 1$	($B = 0.01$)			
Gulf of Suez	1.0	2.0	3.0	0.42×10^{-6} km$^{-0.0}$	0.09	90	90,000
North Sea	0.8	1.8	2.8	0.79×10^{-6} km$^{-0.2}$	0.14	88	56,000
BCFZ	0.9	1.9	2.9	1.55×10^{-6} km$^{-0.1}$	0.36	284	225,000
			$n = 1.46$	($B = 8.91 \times 10^{-3}$ km$^{-0.46}$)			
Gulf of Suez	0.69	1.37	2.05	0.26×10^{-4} km$^{-0.94}$	0.09	90	90,000
North Sea	0.80	1.48	2.17	0.16×10^{-4} km$^{-0.83}$	0.096	143	211,000
BCFZ	0.90	1.58	2.27	0.31×10^{-4} km$^{-0.73}$	0.223	460	948,000

For the Gulf of Suez y_0 and nc_2 are observed and other parameters are derived. For the North Sea and the Badajoz–Cordoba fault zone (BCFZ), a_1 and c_1 are observed and other parameters are derived. δN values are estimated numbers of faults with L = 10, 1 and 0.1 km in each 1000 km^3 of crustal volume, estimated using equation (A3.2) with $k = 0.1$.

strain can be obtained using algebra for cumulative distributions of small faults, even though the true population of small faults is not open-ended, but instead gives way to a population of large faults possibly with a different exponent. Suppose the number N_L of large faults with displacement D or greater in a region with dimensions $W \times J \times H$ is given by

$$N_L(D) = a_L WJHD^{-c}, \quad (16)$$

where a_L and c_L are the number-density and exponent of large faults, analogous to a and c for small faults. Using (1), (16) can be rewritten as

$$N_L(L) = a_L WJHB^{-c}L^{-nc}. \quad (17)$$

Equation (A1.1) gives the number of small faults that would exist in a region if their distribution were open-ended. Use of equation (A1.1) with $L = L_0$, the upper length-limit for small faults (and thus the lower length limit for large faults) would give a notional number of small faults expected with length above L_0, but which do not actually exist. I will call this number N_x. Equation (17) gives the number of large faults with length above L_0, which I will call N_y. The true number of faults with length no greater than L, where $L < L_0$, is thus

$$N = aB^{-c}WJHL^{-nc} + N_y - N_x \quad (18)$$

which will in general differ from the number given by (A1.1) (because N_x and N_y are not necessarily equal). However, if (18) is differentiated, as is required to obtain strain or numbers of small faults in any length range (see Appendices 1 and 3), the contribution from the two constant terms N_y and N_x disappears, and one is left only with the term that is present when (A1.1) is used in its original form. The procedures for estimating W_1, W_2, A_2 and A_3 in Appendix 2 each implicitly assume the population of small faults is open-ended and persists to arbitrarily large L, whereas in reality it is not: it is bounded by a population of large faults.

OBSERVATIONAL CASE STUDIES

The North Sea

Large normal faults in the northern North Sea account for ~20 km of late Jurassic extension across a zone that is ~250 km wide (e.g. Roberts *et al.* 1990). Spatially-averaged Jurassic extensional strain across these faults is thus ~0.09. Because small faults also contribute to local strain, this estimate is a lower bound for the total strain from faulting. Walsh *et al.* (1991) and Marrett & Allmendinger (1992) have suggested that the proportion of extensional strain associated with small faults in the northern North Sea is substantial, perhaps ~60% of the total. However, as already noted they did not estimate the absolute strain associated with these faults.

Walsh *et al.* (1991) analysed normal faults in the North Sea using one-dimensional sampling at several scales. They obtained vertical samples of $N_1(D)$ for $D > 1$ mm using core from boreholes. They compared these with horizontal samples of $N_1(D)$ from seismic profiles on the regional scale and on the scale of individual oilfields, for $D \sim 1$ m to $\gtrsim 1$ km, using a typical fault dip, δ, of ~60°, to convert numbers of faults between the two types of sample. Their regional-scale profiles have $W \cong 250$ km, N_1 (1 km) $\cong 6$ and $c_1 \cong 0.8$, making $a_1 \cong 0.024$ km$^{-0.2}$. With $\delta = 60°$, if $n = 1$ and $B = 0.01$, then $c = 2.8$ and $a = 0.69 \times 10^{-6}$ km$^{-0.2}$. If $n = 1.46$ and $B = 8.91 \times 10^{-3}$ km$^{-0.46}$ instead, then $c = 2.17$, and $a = 1.38 \times 10^{-5}$ km$^{-0.83}$. Consistency between their reported cumulative number of faults and number of faults per unit length of section requires $W \cong 30$ km. For a single profile N_1(0.1 km) is ~5, and with c_1 ~0.8, a_1 is ~0.026 km$^{-0.2}$ For 56 profiles together, N_1(0.1 km) is ~170, so on average for a single profile N_1(0.1 km) is ~3, and a_1 is ~0.016 km$^{-0.2}$. These estimates from local profiles thus bracket the regional value.

Using equation (15), the contribution of faults with L up to L_0 can be estimated for $c_1 = 0.8$ and $a_1 = \sim 0.02$ km$^{-0.2}$. Values of a and other parameters can be estimated using equations from Appendix 1 (Table 3). With $n = 1$ and $B = 0.001$, for $L_0 = 1$ km ($D_0 = 10$ m), ε is ~0.016; for $L_0 = 10$ km ($D_0 = 100$ m), ε is ~0.025. Assuming $n = 1.46$ and $B = 8.91 \times 10^{-3}$ km$^{-0.46}$, for $L_0 = 1$ km ($D_0 = 89$ m) ε is ~0.023; for $L_0 = 10$ km ($D_0 = 257$ m) ε is ~0.030 (Table 4). All these strain estimates are small, no greater than ~0.03 and thus no more than ~30% of the contribution from large faults (Table 4). Only a small fraction of strain in the northern North Sea has thus been taken up by small faults with $L < 10$ km.

Table 4. Strain estimates

	Previous work		This study					
	$\varepsilon_s/\varepsilon_{tot}$ (%)	$\varepsilon_L/\varepsilon_{tot}$ (%)	ε_L	n	ε_s	ε_{tot}	$\varepsilon_s/\varepsilon_{tot}$ (%)	$\varepsilon_L/\varepsilon_{tot}$ (%)
North Sea	~45	~55	0.087	1.46	0.036	0.123	29	71
				1	0.025	0.112	22	78
Suez	~30	~70	0.27	1.46	0.036	0.306	12	88
				1	0.102	0.372	27	73
BCFZ	~60	~40	0.06	1.46	0.36	0.42	86	14
			0.09	1	0.29	0.38	76	24

ε_s and ε_L denote the extensional strains associated with small ($L < 10$ km) and large faults, ε_{tot} ($=\varepsilon_L + \varepsilon_s$) being the overall extensional strain. For the North Sea, estimates from previous work use fig. 4 of Walsh *et al.* (1991), which shows ε_L for faults above each value of D as a function of c_1. Walsh *et al.* (1991) indicated that δ is typically ~60° in the North Sea, so $\sin(2\delta)$ is ~0.87, and supported the use of Marrett & Allmendinger's (1991) equation (with $n = 1.46$) linking L and D, which predicts $D = 0.26$ km for $L = 10$ km. Walsh *et al.* (1991) calculated that this value of D gives $\varepsilon_L = 55\%$ for $c_1 = 0.8$. For the Badajoz–Cordoba fault zone, the estimates from previous work by Jackson & Sanderson (1992) are for proportions of strain accommodated on faults below and above the resolution of Spanish 1:50,000 geological maps. The limit of fault displacement resolution of ~0.1 km roughly matches the transition from small to large faults. For the Gulf of Suez, nc_2 is 2. If n is taken as 1.46, from Marrett & Allmendinger (1991), then c_1 is 0.68. Figure 3 of Walsh *et al.* (1991) gives ε_L ~70% for D ~0.26 km with c_1 ~0.7. The ε_L value from this study for the Gulf of Suez is from summation of heaves. The alternative rigid-domino interpretation gives $\varepsilon_{tot} = 0.23$. My analysis gives $\varepsilon_s = 0.036$ for $n = 1.46$, making $\varepsilon_s/\varepsilon_{tot} = 16\%$ and $\varepsilon_L/\varepsilon_{tot} = 84\%$. With $n = 1$ it gives $\varepsilon_s = 0.102$, making $\varepsilon_s/\varepsilon_{tot} = 44\%$ and $\varepsilon_L/\varepsilon_{tot} = 56\%$.

The Badajoz–Cordoba fault zone

The Badajoz–Cordoba fault zone (BCFZ) is an ancient NW–SE-trending left-lateral fault zone in southern Spain, which is exposed for ~300 km length. During Hercynian time it became cut by SSW-trending left-lateral strike-slip faults, which offset its SE-trending branches leftward, and which mark the last phase of deformation in its vicinity. Jackson & Sanderson (1992) investigated the displacement on these SSW-trending faults. No independent estimate of strain, other than from fault sampling, is available.

Jackson & Sanderson (1992) investigated the power law governing $N_1(D)$, using one-dimensional sampling across profiles on published 1:50,000 maps (each of which appears to cover 40 km length) and more detailed one-dimensional sampling in the field. Their parameter C is equivalent to my $a_1 W$, although they omitted its units. Some of their figures normalize $N_1(D)$ per unit length of sample line: as $N_1(D)/W$ in terms of my notation. The scale factor of this normalized parameter is equivalent to my a_1, and is not—of course—dimensionless. Their fig. 8 shows a one-dimensional sample of $N_1(D)/W$ fit to a single power law with $c_1 = 0.9$ and a_1 ~0.05 km$^{-0.1}$, which fits both their map and field data sets. Their field data appear complete for displacement ~10 mm to ~0.5 m; their map data appear complete for displacement ~50 m to ~1 km. Their observed value of a_1 makes $a = 1.55 \times 10^{-6}$ km$^{-0.1}$ for $n = 1.0$ and $B = 0.01$, or $a = 0.31 \times 10^{-4}$ km$^{-0.73}$ for $n = 1.46$ and $B = 8.91 \times 10^{-3}$ km$^{-0.46}$.

Table 3 indicates that, at all scales examined, the BCFZ is roughly three to four times as pervasively faulted as the North Sea. Treating all the faults sampled as SSW-trending vertical left-lateral faults and neglecting effects of any finite lower size limit, from equation (A1.43) the overall displacement accommodated on all faults with D up to 0.1 km is 0.36 km for each kilometre of along-strike length in the ESE direction, or 107 km throughout the 300 km distance where the BCFZ is exposed (assuming it is all as pervasively faulted as the length that was examined). The left-lateral shear strain associated with these faults is thus ~0.36.

Assuming brittle layer thickness 10 km, with $B = 0.01$ and $n = 1$ the limit $D_0 = 100$ m also marks the limit of small faults, and the strain of ~0.36 calculated above is thus accommodated on small faults. With $B = 8.91 \times 10^{-3}$ km^{-1} and $n = 1.46$, $L = 10$ km corresponds to $D = 257$ m instead. The estimated strain accommodated on small faults rises to ~0.39. On the other hand, c_1 for the BCFZ is sufficiently near 1 that the lower length limit of small faults can affect estimation of strain. Assuming this limit is 1 mm, the absence of smaller faults (below $D_{min} = 0.01$ mm for $n = 1$ or $\sim 1.5 \times 10^{-5}$ mm for $n = 1.46$) will reduce estimated strain by ~0.07 ($n = 1$) or ~0.03 ($n = 1.46$). The estimated strain accommodated on small faults in the BCFZ is thus ~0.29 for $n = 1$ and $B = 0.01$, or 0.36 for $n = 1.46$ and $B = 8.91 \times 10^{-3}$ km$^{-0.46}$.

Faults with D of 0.1–1 km (the upper limit considered by Jackson & Sanderson 1992) will contribute strain ~0.09; faults with D 0.26–1 km will contribute strain ~0.06. Their sampled fault distribution shows evidence that a small number of the very largest faults may have been missed, and thus gives only a lower bound to the strain accommodated on large faults in the BCFZ. Analysis by Jackson & Sanderson (1992) suggested that ~60% of the strain in the BCFZ is accommodated on small faults. My analysis suggests that the proportion may be even higher: perhaps as high as 84% for $n = 1.46$

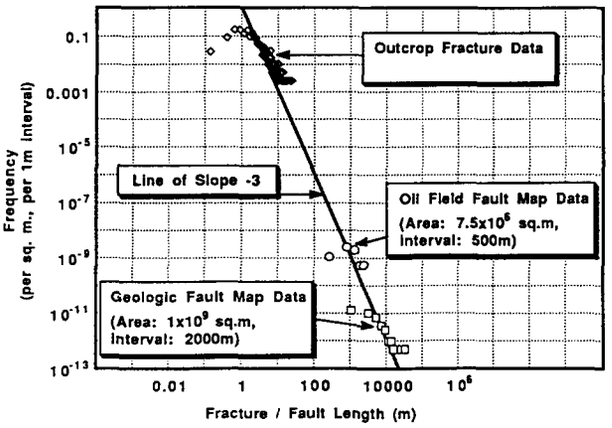

Fig. 1. Logarithmic graph of number density of faults from two-dimensional sampling, $(-1/WJ)\ dN_2(L)/dL$, against L, for normal faults in the Gulf of Suez. Adapted from fig. 2 of Heffer & Bevan (1990). The power law fitted has exponent $-nc_2 - 1 = -3$. As noted in Appendix 1, the parameter plotted in this figure is $nc_2a_2B^{-c_2}L^{-nc_2-1}$, and is 0.9 for $L = 1$ m.

or 76% for $n = 1$. This is because of the close packing of small faults (Table 3), which are thus able to accommodate substantial strain (Table 4).

The Gulf of Suez

The Gulf of Suez is a ~70 km wide zone of SW–NE extension. Extension appears to have begun between late Oligocene and middle Miocene time, at ~25–15 Ma, and continues to the present (e.g. Jackson *et al.* 1988). Two major normal faults southwest of the Gulf have ~35° dip and are ~25 km apart with heave ~5 km and tilt of adjoining beds ~10° (Jackson *et al.* 1988). Rigid domino analysis of these faults gives extension factor sin (45°)/sin (35°) or 1.23, indicating extensional strain ~0.23. On the northeast side of the Gulf, large normal fault zones bounding the coast and up to ~20 km inland have combined heave also ~5 km (e.g. Moustafa 1993). Heaves of the largest normal faults thus indicate extensional strain ~15 km/~55 km or ~0.27. Allowance for other normal faults that cut the brittle layer may increase this estimate. Spacings of and tilt angles around these major normal faults are such that summation of heaves is expected to give greater extensional strain than rigid domino analysis (e.g. Westaway & Kusznir 1993).

Heffer & Bevan (1990) analysed faults in a 1000 km^2 sample area along part of the southwest flank of the Gulf, using two-dimensional sampling from maps and outcrop (Fig. 1). Almost all of their data set is for faults with $L < 10$ km, which most likely means small faults. Figure 1 shows a parameter y plotted against L, such that $y \propto L^{-3}$ or $y = y_0L^{-3}$, where y_0 is a constant of proportionality. Appendix 1 contains the theory needed to determine the three-dimensional population of small faults that is consistent with Fig. 1, enabling it to be compared with the other case study localities that were sampled differently. From Fig. 1, for $L = 1$ m, $y = 0.9$ m^{-3}; hence $y_0 = 0.9$. The -3 exponent in Fig. 1 means that $nc_2 + 1 = 3$ or $nc_2 = 2$. If $n = 1$ then $c_2 = 2$ and thus from equation (4) $c = 3$. Using equation (A1.36) with $n = 1$, $c_2 = 2$, and $B = 0.01$, $y_0 = 0.9$ for $L = 1$ m gives $a_2 = 4.5 \times 10^{-5}$.

Using equation (A1.29), again with $c_2 = 2$, $c = 3$, and $B = 0.01$, $a_2 = 4.5 \times 10^{-5}$ means that $a = 3 \times 10^{-7}$ for $\delta = 90°$. Westaway (1992a) reported this value of a as derived from Heffer & Bevan (1990), but through length limitations was unable to explain how it was obtained. Heffer & Bevan (1990) did not state the typical orientation of small faults in their study area. Given their horizontal sample planes from maps and outcrops, assuming $\delta = 90°$ is equivalent to assuming that they are typically vertical. However, it is probably more realistic to assume that they dip at ~35–45°, like the large normal faults nearby (Jackson *et al.* 1988). With δ typically 45°, a better estimate for a for the Gulf of Suez is thus ~4.2×10^{-7}. With $\delta = 45°$, the largest small fault that can be present has length $L_0 = H/\cos(\delta)$: $L_0 = 10$ km requires $H \sim 7.1$ km.

The tailing-off of numbers of faults in Fig. 1 below $L \sim 1$ m indicates incomplete sampling in the data sets shown. Other data presented by Heffer & Bevan (1990) show that the same distribution, with the -3 exponent, persists to the scale of microfractures with length ~1 mm, giving a lower limit of L, L_{min}, of ~1 mm. For $n = 1$, the strain contribution from small faults in the Gulf of Suez is thus ~0.1.

Using the alternative relation between D and L with $n = 1.46$ and $B = 8.91 \times 10^{-3}$ km$^{-0.46}$, c_2 is 1.37 and a_2, from (16), is 7×10^{-4} km$^{-0.63}$. Using (A1.29), this gives $a = 2.6 \times 10^{-5}$ km$^{-0.94}$. Using (A1.38), the strain contribution from such a population of small faults with $L_0 = 10$ km would thus be 0.036. Note that this relation for $D(L)$ with $n = 1.46$ predicts less strain in the Gulf of Suez than the alternative with $n = 1$.

The Gulf of Suez illustrates the inconsistencies that result when attempts are made to estimate fault spacings from cumulative distributions. Using equation (A2.5), for the two-dimensional sampling by Heffer & Bevan (1990) one fault with length 10 km or greater is expected to occur in sample plane area $A_2 = 222$ km^2. If this area is assumed square, it would have side length ~15 km. If instead it is assumed rectangular with width L_{max}, its length would be 22 km. In contrast, using (A2.2) the length W_1 of a one-dimensional profile needed to find one fault with length 10 km can be estimated as 11 km. With brittle layer thickness $H \sim 7.1$ km and fault dip $\delta = 45°$, from equation (A2.8) one would typically need to sample a 2360 km^3 volume, with surface area of 333 km^2, in order to find one fault of this size. If this surface area is square, it has side length ~18 km. These predicted spacings from one-, two- and three-dimensional sampling thus differ in the ratio $c_1:c_2:c$, as was established earlier to be true in general. The correct estimates in this case are N_2 and a_2, which are obtained directly by sampling.

As Appendix 3 shows, consistent results for numbers and spacings of small faults can be obtained from incremental distributions. With $L_0 = 10$ km and $\delta L = 1$ km, such that k $(=\delta L/L)$ is 0.1, using (A3.13) the

typical area required to find one fault by two-dimensional sampling is 1111 km^2. This k value is chosen so that all faults with length 9–10 km count as 10 km. From the derived three-dimensional fault distribution (equation A3.14), the sample volume required to find one such fault is 7857 km^3, which also means surface area 1111 km^2 given the assumed ~7.1 km thickness of the brittle layer. The typical spacing in any given direction of faults in the length range 9–10 km in the Gulf of Suez can be estimated as the square root of 1111 km^2, or ~30 km. It is thus indeed comparable to the length of these faults.

Comparison of results

Tables 3 and 4 summarize the distribution of small faults and strain estimates for the case study localities. The available data allow c to be estimated precisely, subject to assumed values of n. For all three regions, c is ~2 if n is 1.46, but ~3 if n is 1 instead. For the North Sea and the BCFZ, the two different n values give similar estimates of strain, the larger n value giving somewhat greater strain. The larger n value also indicates a greater number of faults, except for lengths near 10 km. For the Gulf of Suez, the smaller n value gives about three times as much strain as the larger value. Predicted numbers of faults in the Gulf of Suez are independent of n, because the fault sampling was carried out using a method that allows this to be so (see equation A3.16). For $n = 1$, greater numbers of faults are predicted in the Gulf of Suez than in the North Sea; for $n = 1.46$, greater numbers are predicted in the North Sea. Most estimates of strain associated with small faults are ~0.03, except for the value of ~0.1 when $n = 1$ in the Gulf of Suez. The number density of small strike slip faults at each scale in the BCFZ is roughly four times greater than the number densities of small normal faults of the same scale in the two extensional provinces. These results thus support the conclusions of Westaway (1992a,b) that strains of $\gtrsim 0.01$ may be taken up entirely on small faults, but require spacings of the largest small faults comparable to their dimensions. Substantially larger strains presumably require the development of large faults.

Table 4 also compares the proportions of strain taken up on small normal faults estimated in this study with previous estimates for $n = 1.46$ from Walsh *et al.* (1991). I estimate the proportion of the extensional strain in the North Sea that is accommodated on small faults as ~20%, regardless of n. This is a much smaller proportion than has been obtained by Walsh *et al.* (1991) and Marrett & Allmendinger (1992). In the Gulf of Suez, application of the method of Walsh *et al.* (1991) for $n = 1.46$ would predict that ~20% of strain is taken up on small faults. This study predicts that for $n = 1$ the proportion of strain accommodated on small faults is actually much greater, ~40%. In the BCFZ, may estimate of the proportion of strain accommodated on small faults is >70%, even more than was suggested by Jackson & Sanderson (1992).

DISCUSSION

As already noted, previous analyses have assumed that numbers of small and large faults in any given region follow a single self-similar distribution. This assumption leads to the ability to estimate proportions of strain associated with each fault population, without knowledge of the total strain or even of the number-density of faults in either population. My analysis predicts a similar proportion of strain associated with small faults for the Gulf of Suez with $n = 1.46$, compared with the older method. However, the analysis predicts a much smaller proportion of the strain is associated with small normal faults in the North Sea. It is important to consider the significance of these differences. Do they mean that populations of small and large faults are self-similar in some regions but not in others? Do they mean that the uncertainties in both methods are so large that they cover both possibilities, so that it becomes a matter of personal preference which method is used? Or is one method demonstrably wrong in principle?

In Fig. 1, a line with slope −3 has been fitted through small faults with $L < 10$ km and large faults with $L > 10$ km. Both fits seem reasonable. The fit through the small faults indicates $nc_2 + 1 = 3$, requiring $nc_2 = 2$ or $nc = 3$; the fit through the large faults indicates $nc + 1 = 3$, or $nc = 2$. Although both parts of the fitted line have the same slope (Fig. 2a), they thus indicate different exponents c for large and small faults. If one-dimensional sampling of $dN_1(L)/dL$ had been carried out in the Gulf of Suez, the figure would still show an exponent of −3 for $L > 10$ km, indicating $nc = 2$ for large faults, as before. However, for $L < 10$ km the exponent $-nc_1 - 1$ would be −2, indicating $nc_1 = 1$. The graph of sampled numbers of faults would now have an upward kink at $L = 10$ km, when the exponent changes from −2 to −3 (Fig. 2b). Similarly, for three-dimensional sampling the exponent for small faults would be −4, indicating $nc + 1 = 4$ or $nc = 3$. However, the exponent for large faults would still be −3. The graph of sampled numbers of faults would now have a downward kink at $L = 10$ km (Fig. 2c).

Because only a small range of data is available for $L > 10$ km in Fig. 1, one may well not notice the kinks in Figs. 2(b) & (c), but may instead extrapolate the trend through the small faults into the range of L for large faults. Careful inspection of Fig. 1 indicates that Heffer & Bevan (1990) may have unwittingly done this. For $L > 10$ km, their data points appear to diverge above their fitted line, suggesting that the true value of $nc + 1$ for large normal faults in the Gulf of Suez is substantially less than 3, indicating that nc for these faults is substantially less than 2: possibly as low as ~1.

The many plots of $N_1(D)$ for the North Sea in Walsh *et al.* (1991) show exponents uniformly −0.8 across the size range for both small and large faults. For the small faults this exponent means $c_1 = 0.8$, making (for $n = 1$) $c = 2.8$, whereas for the large faults it means $c = 0.8$. If either two- or three-dimensional sampling had been carried out, the difference in exponent would have been obvi-

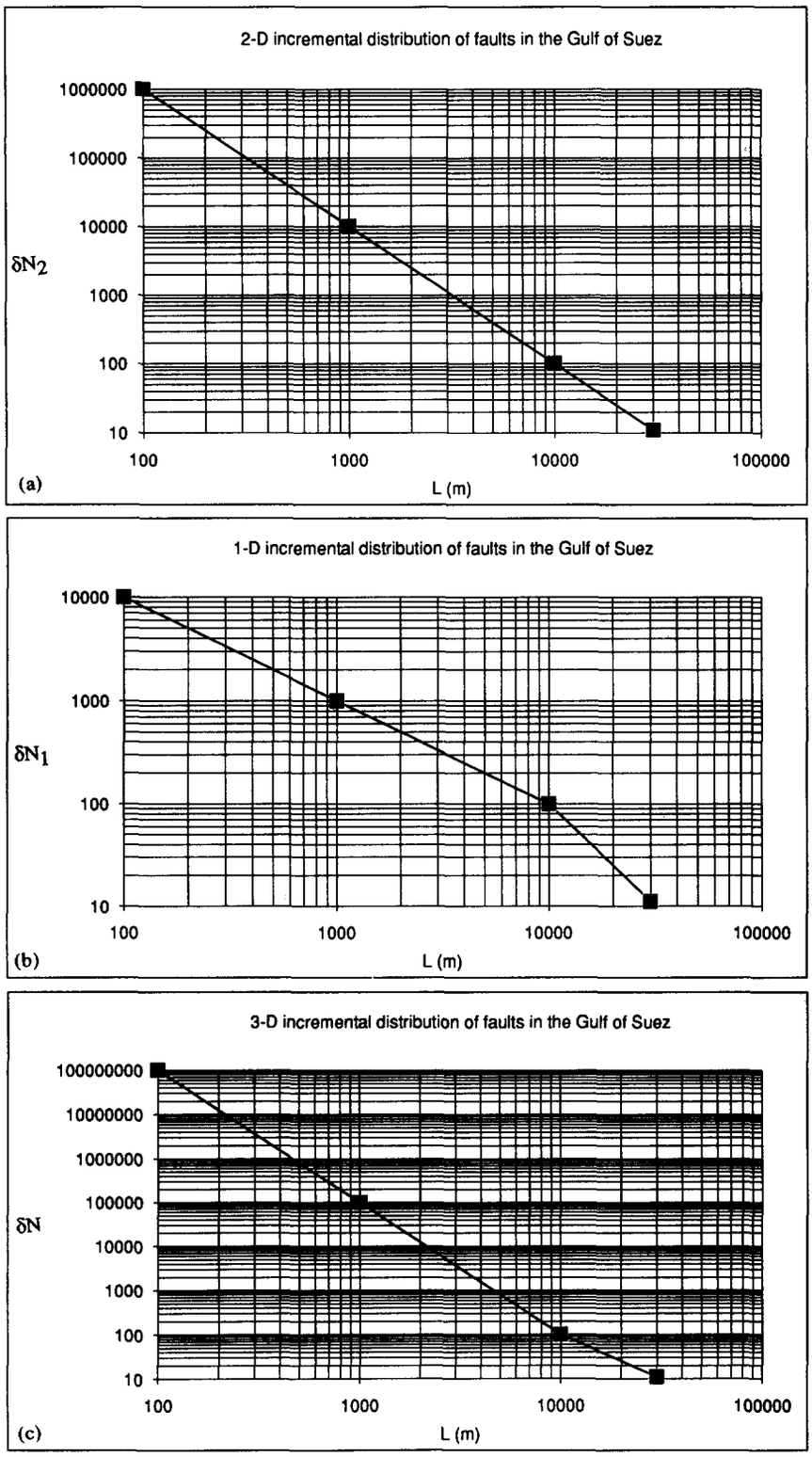

Fig. 2. Logarithmic graphs of incremental distributions of faults in the Gulf of Suez consistent with the fitted line for two-dimensional sampling in Fig. 1. (a) Incremental two-dimensional distribution $\delta N_2(L)$ for $k = 0.1$ in 1.1×10^5 km^2 of two-dimensional area. (b) Incremental one-dimensional distribution $\delta N_1(L)$ for $k = 0.1$ in 1.1×10^4 km of one-dimensional sample length. (c) Incremental three-dimensional distribution $\delta N(L)$ for $k = 0.1$ in 1.1×10^6 km^3 of crustal volume.

ous. Unlike Heffer & Bevan (1990), Walsh *et al.* (1991) show data for more than an order of magnitude range of D for large faults (D from ~100 m to ~4 km). Their data thus support c for large faults close to ~0.8. This is similar to the value for large faults in Japan in Scholz & Cowie (1990), who plotted a distribution of $dN_2(L)dL$ for large faults with exponent $nc + 1 = 2.1$ (for $nc = 1.1$). Populations of large faults may well have substantially smaller exponents (perhaps typically with $c \sim 1$) than small faults (perhaps typically with $c \sim 3$). However, effects of sampling may well frequently cause one- or two-dimensional sample exponents for populations of small faults that are comparable to the three-dimensional exponents for the large faults. This may

well be why the notion that small and large faults follow a single self-similar distribution has arisen.

As already noted, most studies sampling fault populations have presented their results using cumulative distributions, although a few, such as Heffer & Bevan (1990), used incremental distributions instead. The above discussion demonstrates one potential problem with cumulative distributions: the cumulative total of large faults sampled affects the cumulative number of small faults, sometimes making it difficult to separate the two populations. Another significant potential practical difficulty when using cumulative distributions arises through censoring (e.g. Jackson & Sanderson 1992): if a small number of the largest faults in a study area are missed, the cumulative distribution will become skewed down to a much smaller size range of faults, making it difficult to fit a power law. Inspection of Appendix 1 indicates that before any cumulative fault distribution is used to calculate strain, it needs to be differentiated, which in effect means converting it to an incremental distribution. Appendix 3 shows that the same is true if one wishes to use any cumulative distribution to calculate fault spacings. These analyses are greatly simplified, populations of small and large faults with different power laws are more easily isolated, and effects of censoring are avoided, if fault populations are expressed using incremental distributions; no other loss of information results.

CONCLUSIONS

This study derives algebra for quantifying populations of small faults, with length less than the thickness of the brittle layer. This algebra is used to estimate tectonic strain and typical fault spacings, and to interrelate observations from different methods of sampling small faults. Results are listed in Tables 3 and 4 for the three case study regions, the Gulf of Suez, the northern North Sea, and the Badajoz–Cordoba fault zone. This study established that the strain associated with small faults can be determined without any need to assume self-similarity between small and large faults in any given region. Consistent results can be obtained regardless of how the small faults are sampled.

Results differ dramatically from those of previous studies that do assume self-similarity between these two fault populations. For instance, the strain associated with small normal faults in the North Sea is estimated as $\lesssim$20% of the total, in contrast with values of ~40–60% obtained previously. Populations of small and large faults may appear self-similar in a given region when examined using a particular sampling method, but this apparent self-similarity disappears when other methods are used (Fig. 2). The exponent c for the three-dimensional number-density distribution of faults may typically be ~3 for small faults, but appears to be $\gtrsim$1 for large faults instead. Small strike-slip faults in the Badajoz–Cordoba fault zone are roughly four times more closely spaced at each scale than the small normal faults in both extensional provinces considered, and accommodate correspondingly greater strain.

Most recent studies of fault populations have analysed cumulative distributions of faults. This study indicates several important advantages of using incremental distributions instead. In particular, first, it is easier to isolate and treat separately populations of small and large faults that may have different exponents, for example for estimating strain. Second, the equations needed to analyse incremental distributions of faults are typically much simpler than the corresponding forms for cumulative distributions. The equations derived in this study, and the techniques for applying them, will hopefully be of use for analysing populations of faults in other regions that have not yet been studied.

Acknowledgements—Supported in part by Natural Environment Research Council grant GR3/6967 and in part by private funds. I thank Nick Kusznir and Graham Yielding for helpful discussions. Randall Marrett kindly checked my algebra when reviewing an early version of this manuscript. Dave Sanderson and an anonymous reviewer suggested many improvements while reviewing this version.

REFERENCES

Heffer, K. J. & Bevan, T. G. 1990. Scaling relationships in natural fractures: data, theory, and applications. In: *Proc. 2nd European Petroleum Conference*, pp. 367–376. Society of Petroleum Engineers, 367–376 (reprint No. 20981).

Jackson, P. & Sanderson, D. J. 1992. Scaling of fault displacements from the Badajoz–Cordoba shear zone, SW Spain. *Tectonophysics* **210**, 179–190.

Jackson, J. A., White, N. J., Garfunkel, Z. & Anderson, H. 1988. Relations between normal-fault geometry, tilting and vertical motions in extensional terrains: an example from the southern Gulf of Suez. *J. Struct. Geol.* **10**, 155–170.

Kostrov, V. V. 1974. Seismic moment and energy of earthquakes and seismic flow of rock. *Izv. Acad. Sci. USSR Phys. Solid Earth Engl. Transl.* **10**, 23–40.

Kusznir, N. J., Marsden, G. & Egan, S. S. 1991. A flexural cantilever simple shear/pure shear model of continental lithosphere extension: applications to the Jeanne d'Arc Basin, Grand Banks, and the Viking Graben, North Sea. In: *The Geometry of Normal Faults* (edited by Roberts, A. M., Yielding, G. & Freeman, B.). *Spec. Publs geol. Soc. Lond.* **56**, 41–60.

Marrett, R. & Allmendinger, R. W. 1990. Kinematic analysis of fault-slip data. *J. Struct. Geol.* **12**, 973–986.

Marrett, R. & Allmendinger, R. W. 1991. Estimates of strain due to brittle faulting: sampling of fault populations. *J. Struct. Geol.* **13**, 735–738.

Marrett, R. & Allmendinger, R. W. 1992. Amount of extension on "small" faults: an example from the Viking graben. *Geology* **20**, 47–50.

Moustafa, A. R. 1993. Structural characteristics and tectonic evolution of the east-margin blocks of the Suez rift. *Tectonophysics* **223**, 381–399.

Roberts, A. M., Yielding, G. & Badley, M. E. 1990. A kinematic model for the orthogonal opening of the late Jurassic North Sea rift system. In: *Tectonic Evolution of the North Sea Rifts* (edited by Blundell, D. J. & Gibbs, A. D.). Oxford University Press, Oxford.

Scholz, C. H. & Cowie, P. A. 1990. Determination of total geologic strain from faulting. *Nature* **346**, 837–839.

Sornette, D. & Davy, P. 1991. Fault growth model and the universal fault length distribution. *Geophys. Res. Lett.* **18**, 1079–1081.

Walsh, J. J. & Watterson, J. 1987. Distributions of cumulative displacement and seismic slip on a single normal fault surface. *J. Struct. Geol.* **9**, 1039–1046.

Walsh, J. J. & Watterson, J. 1988. Analysis of the relationship between displacements and dimensions of faults. *J. Struct. Geol.* **10**, 239–247.

Walsh, J. J., Watterson, J. & Yielding, G. 1991. The importance of small-scale faulting in regional extension. *Nature* **351**, 391–393.

Westaway, R. 1992a. Evidence for anomalous earthquake size distributions in regions of minimal strain. *Geophys. Res. Lett.* **19**, 1499–1502.

Westaway, R. 1992b. Seismic moment summation for historical earthquakes in Italy: tectonic implications. *J. geophys. Res.* **97**, 15,437–15464. (Correction: *J. geophys. Res.* **98**, 4539, 1993.)

Westaway, R. & Kusznir, N. J. 1993. Fault and bed 'rotation' during continental extension: block rotation or vertical shear? *J. Struct. Geol.* **15**, 753–770. Correction: *J. Struct. Geol.* **15**, 1391.

Ziegler, P. A. 1983. Crustal thinning and subsidence in the North Sea. *Nature* **304**, 561.

APPENDIX 1
GEOMETRIC MOMENT AND STRAIN FOR SMALL FAULTS

Three-dimensional distributions of small faults

Assuming equation (2) describes the number N of faults with displacement no less than D, N can be written using (1) as a function of L as

$$N = aB^{-c}WJHL^{-nc}. \quad \text{(A1.1)}$$

Thus

$$dN/dL = -aB^{-c}cnWJHL^{-1-nc}. \quad \text{(A1.2)}$$

Cumulative geometric moment ΣM_g equals $\int -dN/dL M_g(L)\, dL$. Thus, using (A1.2)

$$\Sigma M_g = \int aB^{-c}cnWJHL^{1+n-nc}dL \quad \text{(A1.3)}$$

with integration limits L_{min} to L_0 covering the length range of the population of small faults.

Provided $n - nc$ does not equal -2, (A1.3) integrates to

$$\Sigma M_g = \frac{aB^{1-c}cnWJH(L_0^{2+n-nc} - L_{min}^{2+n-nc})}{2 + n - nc}. \quad \text{(A1.4)}$$

ΣM_g is thus finite regardless of L_0 and L_{min}, and if $2 + n - nc$ is positive, as is expected, the effect of the lower limits of integration will be minimal.

If $n - nc$ equals -2, or

$$n = 2/(c - 1), \quad \text{(A1.5)}$$

(A1.3) integrates instead to

$$\Sigma M_g = aB^{1-c}cnWJH \ln (L_0/L_{min}). \quad \text{(A1.6)}$$

With $n = 1$ this requires $c = 3$, such that $nc = 3$; with $n = 1.46$ it requires $c = 2.37$, such that $nc = 3.46$. In this case for ΣM_g to remain finite requires L_{min} non-zero.

Geometric moment can be converted to strain using equation (11). Equations (A1.4) and (A1.6) give

$$\varepsilon = \frac{aB^{1-c}cn \sin (2\delta)[L_0^{2+n-nc} - L_{min}^{2+n-nc}]}{2(2 + n - nc)} \quad \text{(A1.7)}$$

and

$$\varepsilon = \frac{aB^{1-c}cn \sin (2\delta) \ln (L_0/L_{min})}{2}. \quad \text{(A1.8)}$$

One-dimensional samples

Suppose that in one-dimensional sampling of profile length W one obtains

$$N_1(D) = a_1WD^{-c_1}, \quad \text{(A1.9)}$$

where a_1 has dimensions of length to the power of $c_1 - 1$. Differentiating gives the number of faults with displacement D in the one-dimensional sample:

$$dN_1/dD = -c_1a_1WD^{-1-c_1}. \quad \text{(A1.10)}$$

Let H and J denote the dimensions, in directions perpendicular to the sample line, of the volume from which the sample is derived. Assuming the sampled faults are equidimensional and randomly distributed in three dimensions, the probability that any given fault is sampled is $p_1(D) = p_1(L) = L^2/HJ$ if its orientation is perpendicular to the sample line. If the typical orientation of the fault planes makes an angle θ relative to the direction in which J is measured, and makes an angle δ relative to the normal to the direction in which H is measured, then the area of the fault plane projected into the direction perpendicular to the sample line is $L^2 \cos(\theta) \sin(\delta)$, and the probability that a given fault is sampled becomes

$$p_1(D) = p_1(L) = L^2 \cos(\theta) \sin(\delta)/HJ. \quad \text{(A1.11)}$$

Thus

$$dN_1(D)/dD = dN(D)/dD\, p_1(D). \quad \text{(A1.12)}$$

Differentiating (2) gives:

$$dN/dD = -caWJHD^{-1-c}. \quad \text{(A1.13)}$$

Using (A1.10), (A1.12) and (A1.13), this gives

$$a_1c_1D^{-c_1} = ac \cos(\theta) \sin(\delta)\, B^{-2/n}\, D^{-c+2/n}. \quad \text{(A1.14)}$$

Thus,

$$c_1 = c - 2/n \quad \text{(A1.15)}$$

(as shown by Marrett & Allmendinger 1991), and

$$a = a_1B^{2/n}c_1/[c \cos(\theta) \sin(\delta)]. \quad \text{(A1.16)}$$

Note that, if length is in metres, a has units m^{c-3}; a_1 has units m^{c_1-1} or $m^{c-2/n-1}$; B has units m^{1-n}, and $B^{2/n}$ thus has units $m^{2/n-2}$. Thus, $a_1B^{2/n}$ has units $m^{c-2/n-1+2/n-2}$ or m^{c-3}, the same units as a. Equation (A1.16) is thus dimensionally consistent. All fractional powers of length cancel when quantities are substituted into (A1.7) to estimate strain. Note also that for (A1.8) to describe strain requires $c_1 = 1$ regardless of n.

By substituting from (1), (A1.14) and (A1.15), given that $\sin(2\delta) = 2 \sin(\delta) \cos(\delta)$, equations (A1.7) and (A1.8) become

$$\varepsilon = \frac{a_1c_1 \cos(\delta)[D_0^{1-c_1} - D_{min}^{1-c_1}]}{(1 - c_1) \cos(\theta)} \quad \text{(A1.17)}$$

and:

$$\varepsilon = \frac{a_1c_1B^{1-c_1} \cos(\delta) \ln (D_0/D_{min})}{\cos(\theta)}. \quad \text{(A1.18)}$$

However, from (A1.5), when (A1.18) is applicable

$$c_1 = c - 2/n = 2/n + 1 - 2/n = 1. \quad \text{(A1.19)}$$

Thus $1 - c_1 = 0$, and (A1.18) simplifies to:

$$\varepsilon = \frac{a_1 \cos(\delta) \ln (D_0/D_{min})}{\cos(\theta)}. \quad \text{(A1.20)}$$

From (A1.9), a_1 has units of metres to the power of $c - 3 - (2/n)(1 - n)$, which are dimensionless when c and n are related via (A1.5). Equation (A1.20) is thus dimensionally consistent.

Whether (A1.17) and (A1.20) are more convenient than (A1.6) and (A1.8) depends on which parameters one knows: if a_1 and c_1 are obtained from one-dimensional sampling and D_0 and D_{min} are known independently, then (A1.17) or (A1.20) is probably the more useful. If a_1 and c_1 are known independently but D_0 and D_{min} are not, the most convenient forms are probably:

$$\varepsilon = \frac{a_1c_1B^{1-c_1} \cos(\delta)[L_0^{n(1-c_1)} - L_{min}^{n(1-c_1)}]}{\cos(\theta)} \quad \text{(A1.21)}$$

and

$$\varepsilon = \frac{a_1n \sin(\delta) \ln (L_0/L_{min})}{\cos(\theta)}. \quad \text{(A1.22)}$$

Two-dimensional samples

Suppose the three-dimensional distribution of small faults in a region follows equation (2). In two-dimensional sampling of the region, which has dimensions W and J in the sampling plane, one will obtain

$$N_2(D) = a_2WJD^{-c_2}. \quad \text{(A1.23)}$$

where N_2 is the number of faults with displacement no less then D.

Differentiating (A1.23) gives the number of faults with displacement D observed in two-dimensional sampling:

$$dN_2/dD = -c_2a_2WJD^{-1-c_2}. \quad \text{(A1.24)}$$

Assuming all small faults are equidimensional, the probability that any given small fault is sampled is $p_2(D) = p_2(L) = L/H$ if the faults are typically oriented perpendicular to the sampling plane, where H is the width of the sampled volume in this perpendicular direction. If faults are typically oriented at angle δ to the sampling plane, the typical length of fault perpendicular to the sampling plane is $L \sin(\delta)$, and the probability that it is sampled becomes

$$p_2(D) = p_2(L) = L \sin(\delta)/H. \quad \text{(A1.25)}$$

Thus

$$dN_2(D)/dD = dN(D)/dD\ p_2(D). \quad \text{(A1.26)}$$

Combining (A1.14) and (A1.26) gives

$$a_2c_2D^{-c_2} = ac \sin(\delta)B^{-1/n}D^{-c+1/n}. \quad \text{(A1.27)}$$

Thus,

$$c_2 = c - 1/n \quad \text{(A1.28)}$$

and

$$a = a_2B^{1/n}c_2/(c \sin(\delta)). \quad \text{(A1.29)}$$

Similar results to (A1.17), (A1.20), (A1.21) and (A1.22) can be derived for two-dimensional sampling. Combining (A1.5) and (A1.16) gives:

$$n = 1/(c_2 - 1) \quad \text{(A1.30)}$$

as the condition for (A1.8) to describe strain.

The above equations for strain can be written in many forms, as for one-dimensional sampling. Probably the most useful are:

$$\varepsilon = \frac{a_2c_2B^{1-c_2}\cos(\delta)[L_0^{(1+n-nc_2)} - L_{\min}^{(1+n-nc_2)}]}{(1+n-nc_2)} \quad \text{(A1.31)}$$

for (A1.7) and

$$\varepsilon = a_2c_2nB^{1-c_2}\cos(\delta)\ln(L_0/L_{\min}) \quad \text{(A1.32)}$$

for (A1.8). They do not simplify as much as the one-dimensional equations, and their dependence on B and n is more explicit. This is because there is no unique value of c_2 where either (A1.31) or (A1.32) describes strain, unlike for one-dimensional sampling where (A1.8) is applicable when $c_1 = 1$.

One may obtain a two-dimensional sample $N_2(L)$ instead of $N_2(D)$. Assuming $D = BL^n$,

$$N_2(L) = a_2WJB^{-c_2}L^{-nc_2}. \quad \text{(A1.33)}$$

One may also obtain a two-dimensional incremental sample dN_2/dL, where

$$\frac{dN_2}{dL} = -nc_2a_2WJB^{-c_2}L^{-nc_2-1}. \quad \text{(A1.34)}$$

The parameter y in Fig. 1 is $(-1/WJ)\ dN_2/dL$, so

$$y = nc_2a_2B^{-c_2}L^{-nc_2-1}. \quad \text{(A1.35)}$$

If y is expressed as $y = y_0L^{-nc_2-1}$ (or $y = y_0L^{-nc}$) then

$$y_0 = nc_2a_2B^{-c_2}. \quad \text{(A1.36)}$$

The units of y_0 will be m^{nc_2-2} or m^{nc-3}; they are dimensionless when $nc_2 = 2$ (or $nc = 3$).

Comparison of equations

Substituting between (A1.29) and (A1.36), the general relation between y_0 and a is simply expressed as:

$$a = y_0B^c/[nc \sin(\delta)]. \quad \text{(A1.37)}$$

Substituting using (A1.29) and (A1.37) gives

$$\varepsilon = \frac{y_0B\cos(\delta)[L_0^{2+n-nc} - L_{\min}^{2+n-nc}]}{(2+n-nc)} \quad \text{(A1.38)}$$

for (A1.7) and

$$\varepsilon = y_0B\cos(\delta)\ln(L_0/L_{\min}) \quad \text{(A1.39)}$$

for (A1.8). These seem to be the simplest forms in which strain can be expressed. The units of y_0B are m^{nc-3} or m^{nc-2-n}, which simplify to m^{nc_1-n} using (A1.19). Because (A1.39) is only applicable when $c_1 = 1$, the units of ε are dimensionless, as is required. Equation (A1.39) is thus dimensionally consistent.

At first sight, (A1.22) appears to be the simplest form of all, as it does not depend explicitly on B. However, by substituting between (A1.36) and (A1.16), a_1 can be expressed in terms of y_0 as

$$a_1 = y_0\cos(\theta)\ B^{c_1}/(nc_1). \quad \text{(A1.40)}$$

If this substitution is made, recalling that (A1.22) is only valid with $c_1 = 1$, (A1.22) can easily be shown to be equivalent to (A1.39); it does indeed depend on B.

One-dimensional sampling for fault displacement

Consider a one-dimensional cumulative sampling $N_1(D)$, along a profile with length W, of a population of faults which follows equation (A1.9). The total displacement on the faults with individual displacement between D and $D + dD$ is $(-dN_1/dD)D\ dD$. The overall displacement across faults with individual displacement between $D_{\min}$ and D_0 is thus

$$\Sigma D = \int_{D_{\min}}^{D_0} (dN_1/dD)D\ dD \quad \text{(A1.41)}$$

$$= \int_{D_{\min}}^{D_0} a_1c_1WD^{-c_1}\ dD. \quad \text{(A1.42)}$$

Thus

$$\Sigma D = \frac{a_1c_1W}{1-c_1}(D_0^{1-c_1} - D_{\min}^{1-c_1}) \quad \text{(A1.43)}$$

for $c_1 < 1$ and

$$\Sigma D = a_1c_1W\ln(D_0/D_{\min}) \quad \text{(A1.44)}$$

for $c_1 = 1$. The overall displacement is proportional to the length of profile, as is expected. Note that in these cases it does not matter whether the faults cut the brittle layer.

For a profile parallel to the extension direction across a set of normal faults with dip δ and extension perpendicular to strike (i.e. $\theta = 0°$) provided $\Sigma D \ll W$, the extensional strain ε is approximately given by $\Sigma D \cos(\delta)/W$. Thus for (A1.43),

$$\varepsilon = \frac{a_1c_1\cos(\delta)}{1-c_1}(D_0^{1-c_1} - D_{\min}^{1-c_1}) \quad \text{(A1.45)}$$

and is consistent with (A1.17).

Equations (A1.17) and (A1.45) do not depend explicitly on B or n. It is thus possible to estimate the strain contribution of (or overall displacement across) a set of small faults up to an arbitrary displacement limit D_0 using only the results of one-dimensional sampling, without assuming any particular relation between D and L. However, to estimate the contribution of the entire population of small faults, one needs to know the value of D_0 for the largest small fault, which has length L_0, which requires the relation between D and L. To make this explicit, one can substitute (A1.17) using (1), to get

$$\varepsilon = \frac{a_1c_1\cos(\delta)B^{1-c_1}[L_0^{1-c_1} - L_{\min}^{1-c_1}]}{(1-c_1)\cos(\theta)}. \quad \text{(A1.46)}$$

Where D_0 is constrained via L_0, equation (A1.17) thus also depends on B.

APPENDIX 2
COMPARISONS OF SAMPLING METHODS FOR CUMULATIVE DISTRIBUTIONS

This Appendix compares predictions of fault spacings based on different methods of sampling cumulative fault distributions.

Numbers of faults with length L or above found by one-dimensional sampling along a line with length W_1 are given by (A1.9). The length needed to be sampled to encounter one fault with length L_0 is thus

$$W_1 = B^{c_1}L_0^{nc_1}a_1^{-1} \quad \text{(A2.1)}$$

which can be rearranged using (A1.16) and (A1.37) to give

$$W_1 = L_0^{nc_1} nc_1/[y_0 \cos(\theta)]. \quad \text{(A2.2)}$$

From (2) and (A1.23), for two-dimensional sampling of an area $A_2 = W_2 J_2$ in a horizontal plane,

$$N_2(L) = a_2 W_2 J_2 B^{-c_2} L^{-nc_2}. \quad \text{(A2.3)}$$

$N_2(L_{max}) = 1$ corresponds to

$$A_2 = L_0^{nc_2} B^{c_2} a_2^{-1}. \quad \text{(A2.4)}$$

Using (A1.37), (A2.4) can be rewritten as

$$A_2 = L_0^{nc_2}(nc_2/y_0). \quad \text{(A2.5)}$$

If as before faults typically make an angle θ relative to the width direction of the sampled area, and this width J_2 is equated to the projected length of the largest fault plane in this direction, $L_0 \cos(\theta)$, then W_2 provides an estimate of the length of the area that typically needs to be sampled to find one fault with length L_0. Making this substitution, (A2.3) becomes:

$$W_2 = L_0^{nc_2} nc_2/[L_0 y_0 \cos(\theta)] \quad \text{(A2.6)}$$

or, from (A1.15),

$$W_2 = L_0^{nc_1} nc_2/[y_0 \cos(\theta)]. \quad \text{(A2.7)}$$

W_2 estimated using (A2.7) is thus c_2/c_1 times W_1 estimated using (A2.2).

A three-dimensional distribution of small faults can be regarded as situated in a volume of upper crust $V = WJH$, where H is the thickness of the brittle upper crust. Let $A_3 = WJ$ denote the horizontal cross-sectional area of this volume. For a three-dimensional distribution of small faults that follows equation (A1.1), the largest fault has $L = L_{max}$ and corresponds to $N(L_{max}) = 1$. From equation (A1.1), the value of V that typically contains one such fault is

$$V = A_3 H = L_0^{nc} B^c a^{-1}. \quad \text{(A2.8)}$$

From (A2.1),

$$A_3 = \frac{L_0^{nc} B^c}{Ha}. \quad \text{(A2.9)}$$

Setting $H = L_{max} \cos(\delta)$ and using (A1.29) and (A1.37), a can be substituted for y_0 to give

$$A_3 = L_0^{nc_2}(nc/y_0). \quad \text{(A2.10)}$$

A_3 from (A2.10) is thus c/c_2 times A_2 from (A2.5).

The above analysis indicates that this approach to comparing methods of fault sampling leads to a major problem. Estimates for typical sizes of volumes and areas expected to contain one fault of a given length L_{max} depend on the sampling method. Suppose two-dimensional sampling is carried out over a plane with area WJ. From two-dimensional sampling, the number N_2 of faults expected with length equal to or greater than $L_{max} = H/\sin(\delta)$, where H is the brittle layer thickness, is

$$N_2(L_0) = a_2 WJB^{-c_2} L_0^{-nc_2}. \quad \text{(A2.11)}$$

Using (A1.29), this can be rearranged to give

$$N_2(L_0) = aWJB^{-c} L_0^{-nc_2} \sin(\delta)\, c/c_2. \quad \text{(A2.12)}$$

From three-dimensional sampling of a volume WJH, the number of faults with length equal to or greater than L_0 would be

$$N(L_0) = aWJHB^{-c} L_0^{-nc}. \quad \text{(A2.13)}$$

Given that $L_0 = H/\sin(\delta)$,

$$N(L_0) = aWJB^{-c} L_0^{-nc_2} \sin(\delta) \quad \text{(A2.14)}$$

which differs from N_2 by a factor c/c_2. Because faults with length L_0 or greater cut the brittle layer, all should be sampled in two-dimensional sampling. One would thus expect N and N_2 in this case to be equal. The fact that they are unequal indicates inconsistency in the method.

This problem arises because the algebra treats all faults in the sampled region as though they were small faults. However, if the distribution of faults is assumed to be open-ended then a finite number will have length L_0 or greater. When numbers of faults are evaluated for different dimensionalities of sampling, the algebra in use implicitly incorporates sampling probabilities for faults of all sizes. These probabilities are less than 1, and are thus meaningful, for faults with length less than L_0. However, when L is greater than L_0, sampling probabilities determined using (A1.11) or (A1.25) are greater than 1, and are thus not meaningful. Appendix 3 shows that this problem can be avoided by working using incremental fault distributions, enabling valid estimates to be made of the spacings of faults of any given size.

APPENDIX 3
COMPARISONS OF SAMPLING METHODS FOR INCREMENTAL DISTRIBUTIONS

Appendix 2 showed that inconsistencies arise when numbers of small faults predicted from cumulative distributions are compared. In this Appendix results are derived for incremental distributions instead, and are shown to be consistent.

Consider a three-dimensional distribution of fault that obeys (2). The number of faults with length L in volume WJH is given by

$$-\frac{dN}{dL} = aWJHncB^{-c} L^{-nc-1}. \quad \text{(A3.1)}$$

Let δN denote the number of faults in the length range δL about L, where $\delta L = kL$, k being small. Thus:

$$\delta N = akWJHncB^{-c} L^{-nc}. \quad \text{(A3.2)}$$

Consider a two-dimensional distribution of small faults that obeys (A1.33). Substituting the small increments δN_2 for dN_2 and $\delta L = kL$ for dL,

$$\delta N_2 = kWJnc_2 a_2 B^{-c_2} L^{-nc_2}. \quad \text{(A3.3)}$$

Substituting for a_2 using (A1.36):

$$\delta N_2 = kWJy_0 L^{-nc_2}. \quad \text{(A3.4)}$$

Substituting instead for a_2 using (A1.29),

$$\delta N_2 = kWJncaB^{-c} L^{-nc}[L \sin(\delta)], \quad \text{(A3.5)}$$

which simplifies, using (A1.25), to

$$\delta N_2 = kWJHp_2(L)ncaB^{-c} L^{-nc}. \quad \text{(A3.6)}$$

Comparison of (A3.2) and (A3.6) gives

$$\delta N_2 = p_2(L)\delta N \quad \text{(A3.7)}$$

consistent with the definition of p_2 in Appendix 1.

Consider a one-dimensional distribution of faults that obeys (A1.9). For this distribution,

$$\frac{dN_1}{dL} = -a_1 Wnc_1 B^{-c_1} L^{-nc_1-1}. \quad \text{(A3.8)}$$

As before, let δN_1 denote the number of faults in the length range δL about L, where $\delta L = kL$, k being small. Thus:

$$\delta N_1 = a_1 kWnc_1 B^{-c_1} L^{-nc_1}. \quad \text{(A3.9)}$$

Substituting for a_1 using (A1.16) gives

$$\delta N_1 = kWncaB^{-c} L^{-nc}[L^2 \cos(\theta) \sin(\delta)]. \quad \text{(A3.10)}$$

This simplifies using (A1.11), to

$$\delta N_1 = kWJp_1(L)ncaB^{-c} L^{-nc}. \quad \text{(A3.11)}$$

Comparison of (A3.2) and (A3.11) gives

$$\delta N_1 = p_1(L)\delta N, \quad \text{(A3.12)}$$

consistent with the definition of p_1 in Appendix 1.

Using (A3.3), the typical area $A = WJ$ that needs to be sampled to find one fault with length L_0, for which $p_2 = 1$, can be estimated, by setting $\delta N_2 = 1$, as

$$A = WJ = B^{c_2} L_0^{nc_2}/[knc_2 a_2]. \quad \text{(A3.13)}$$

Using (A3.2), the typical volume $V = WJH$ that needs to be sampled to find one fault with length L_{max} can be estimated, by setting $\delta N = 1$, as

$$V = WJH = B^c L_0^{nc}/[knca]. \quad \text{(A3.14)}$$

By substituting using (A1.29), it can easily be shown that (A3.13) and

(A3.14) are always consistent. One potentially useful form into which (A3.13) can be arranged is

$$A = WJ = B^c L_0^{nc_2}/[knca \sin(\delta)]. \quad \text{(A3.15)}$$

Finally, substituting using (1), (A1.29) and (A1.36), equation (A3.2) can be converted to

$$\delta N = y_0 kWJHL^{-nc}/\sin(\delta). \quad \text{(A3.16)}$$

Equation (A3.16) shows that if y_0 and nc are observed from two-dimensional incremental samples of fault lengths, then numbers of faults around any given length can be determined independently of the parameters B and n that define the relation between D and L. The same is not necessarily true if other sampling methods are used. Equations (A3.3) and (A3.9) clearly depend on n and B, and indicate that numbers of faults around any given length cannot uniquely be determined from either one- or two-dimensional samples of cumulative distributions of fault numbers against L. Rearranging these equations in terms of D gives

$$\delta N_1 = a_1 kWnc_1 D^{-c_1} \quad \text{(A3.17)}$$

for the one-dimensional equation (A3.9) and

$$\delta N_2 = kWJnc_2 a_2 D^{-c_2} \quad \text{(A3.18)}$$

for the two-dimensional equation (A3.3). One-dimensional (or two-dimensional) samples of cumulative numbers of faults against D can give directly a_1 and c_1 (or a_2 and c_2), but independent information about n is required to determine numbers of faults in any given displacement range.